Signal Processing 201 (2022) 108702

Contents lists available at ScienceDirect

Signal Processing

journal homepage: www.elsevier.com/locate/sigpro

On the positivity of Teager-Kaiser's energy operator

Yves Préaux[a], Abdel-O. Boudraa[a,*], Kieran G. Larkin[b]

[a] Ecole Navale/Arts et Metiers Institute of Technology, IRENav, BCRM Brest, CC 600, 29240 BREST Cedex 9, France
[b] Nontrivialzeros Research, 22 Mitchell Street, Putney,NSW 2112, Australia

ARTICLE INFO

Article history:
Received 26 September 2021
Revised 24 May 2022
Accepted 19 July 2022
Available online 25 July 2022

Keywords:
Teager-Kaiser energy operator
Positivity of Teager-Kaiser energy operator
AM-FM signal
Instantaneous frequency
Instantaneous amplitude
Initial phase of a signal

ABSTRACT

This paper is devoted to the problem of positivity conditions of Teager-Kaiser energy operator in one dimension. This operator and its extended versions form a class of energy operators that are well adapted for non-stationary signals and images processing and thus, are well suitable for a large range of domains and applications. However, negativity of the operator is essentially meaningfulness and thus prevents it from having some useful mathematical properties. We tackle this problem of positivity, and we show that it can be formulated logarithmically in terms of attenuation and phase of the input signal, rather than the more conventional AM-FM model. A more detailed analysis of the positivity conditions of the operator is presented, which extends and generalizes the findings reported in the literature. We highlight the existence of a critical interval over which the positivity is depending on the initial phase of the input signal. Outside this critical interval, the positivity is guaranteed. Positivity conditions are illustrated and analyzed on synthetic and real signals.

1. Introduction

A large class of real signals are found to be non-stationary in nature, where their amplitude envelope and frequency content are time varying. Signal representations that are inherently able of capturing such non-stationarity are of great practical interest in many areas of signal and images processing applications. A well known model for decomposing a non-stationary signal into its essential components, is the amplitude-modulation frequency-modulation (AM-FM) model which describes the signal content in terms of amplitude and phase functions. The basic problem in processing AM-FM signals is the demodulation, i.e., estimation of the information stored in the instantaneous amplitude (IA) and instantaneous frequency (IF) of the input signal. These physically meaningful features, are well suited for characterizing non-stationary signals. The development of the nonlinear Teager-Kaiser (TK) energy operator has facilitated the energy representation and demodulation of signals modeled by AM-FM functions. TK energy operator is a non-linear signal operator introduced by Teager [1,2], and formalized and its properties explored by Kaiser [3,4]. This operator owes its energetic properties to the fact that, when it is applied to an harmonic oscillator output (mass-spring oscillator of constant stiffness), it tracks the energy (per half unit mass) of a source generating the signal [5–9]. Continuous version of this operator, noted $\Psi_c(.)$, when applied to a signal $x(t)$ is given by

$$\Psi_c\big(x(t)\big) = \dot{x}^2(t) - x(t)\ddot{x}(t) \tag{1}$$

where $\dot{x}(t)$ and $\ddot{x}(t)$ are respectively the first and second derivatives of $x(t)$ with respect to time t. Discrete-time and scaled counterpart of $\Psi_c\big(x(t)\big)$ is derived by replacing $x(t)$ by $x(n) = x(nT_e)$, where T_e is the sampling period, and derivatives $\dot{x}(t)$ and $\ddot{x}(t)$ by finite differences:

$$\mathrm{TK}_d(x(n)) = x^2(n) - x(n-1)x(n+1),\ n \in \mathbb{N} \tag{2}$$

The fact the operator spans three adjacent samples only of $x(t)$, highlights its superior localization property. This input-output relation is termed as "Teager's algorithm" [3]. A striking feature of $\Psi_c(.)$ is its behavior, when applied to AM-FM signal $x(t)$ of the form [11–13]:

$$x(t) = a(t)\cos\big(\phi(t)\big) \tag{3}$$

where $a(t)$ is the IA, a positive function corresponding to the information to be transmitted [10], and $\phi(t)$ denotes the instantaneous phase of $x(t)$. The TK energy operator applied to AM-FM signal $x(t)$, and its first derivative yield respectively

$$\Psi_c\big(x(t)\big) \simeq a^2(t)\dot{\phi}^2(t) \tag{4}$$

$$\Psi_c\big(\dot{x}(t)\big) \simeq a^2(t)\dot{\phi}^4(t) \tag{5}$$

Approximations (4) and (5) are valid under certain general realistic constraints that restrict the bandwidths of $a(t)$, $\dot{\phi}(t)/2\pi$ and the

* Corresponding author.
E-mail addresses: yves.preaux@ecole-navale.fr (Y. Préaux), boudra@ecole-navale.fr (Abdel-O. Boudraa), spiralphase@yahoo.com.au (K.G. Larkin).

https://doi.org/10.1016/j.sigpro.2022.108702
0165-1684/

maximum frequency deviation of the FM component to be much smaller than the carrier frequency of $x(t)$ [5]. Output of $\Psi_c\big(x(t)\big)$ is approximately the squared product of the IA and IF of $x(t)$, and thus it can be termed as frequency weighted energy. Under the assumption that the operator outputs (4) and (5) are positive, this has motivated the continuous energy separation algorithm (ESA) which provides at each instant estimates of the time-varying IF, $f(t)$, and of IA, $|a(t)|$, of $x(t)$ [5]:

$$f(t) \simeq \frac{1}{2\pi}\sqrt{\frac{\Psi_c[\dot{x}(t)]}{\Psi_c[x(t)]}} \tag{6}$$

$$|a(t)| \simeq \frac{\Psi_c[x(t)]}{\sqrt{\Psi_c[\dot{x}(t)]}} \tag{7}$$

ESA highlights the fact that $\Psi_c(.)$ is instantaneous and able to respond very quickly to changes in IA and IF of $x(t)$. This is why $\Psi_c(.)$ is well adapted for demodulation and formant tracking.

The very low computational complexity of the operator, and its sensitivity to instantaneous changes in frequency-dependent energy of the input signal, have motivated a lot of research works in different domains such as AM-FM demodulation [14–21], speech analysis [22–29] signal detection [30–37], time-delay estimation [33], time-frequency analysis [38–41] and image processing [42–45], to name a few. For more details and for general papers on this topic, the reader can refer to the overview on TK energy operator and its applications presented in [46]. Since TK energy operator can track the energy of linear oscillator, it is viewed an energy operator and thus, all the TK-based studies and applications, reported in the literature, work under the basic assumption that the operator outputs are positive. In absence of a deep study addressing the positivity problem of the operator, negative values of the operator are mostly attributed to noise, derivative discretization schemes or to roundoff errors involved in the numerical calculations of the operator. Consequently, often we make sure the output of the operator is non-negative, and a way out is to use the absolute function.

Although there are a lot of research works done in the domain of TK energy operator and its extensions till now, there are few works in the literature that address the challenging problem of the positivity of the operator $\Psi_c(.)$. This issue has been first addressed by Margos et al. [22] and later positivity solutions on simplest signals namely, linear signals, sinusoidal signals and exponential of order one have been discussed by Bovik and Margos [47]. They proposed a general solution but it still limited to a "sufficiently smooth" signal amplitude defined by the signal's logarithmic concavity [47]. Their study was later supplemented by Larkin in the case of AM-FM signal [48]. Recently, positivity problem has also been discussed by Banerjee and Chakrabarti but their study is still limited to harmonique signals [49].

Positivity underpins the definition of an ideal energy operator - a negative energy signal is essentially meaningless- but $\Psi_c(.)$ only approximates the ideal [48]. The positivity of idealized version of $\Psi_c(.)$ is guaranteed because the output is a square function:

$$\Psi_c\big(x(t)\big) = a^2(t)\dot{\phi}^2(t) \tag{8}$$

The positivity of $\Psi_c(.)$ is required because TK-based tools and applications only work under positivity assumption of $\Psi_c(.)$. One can quote situations or tools based on the positivity assumption of the operator [46]:

1. Interpretation as some physical energy quantity of $\Psi_c(.)$ and its extension versions such as higher order (HO) differential energy operators [20], generalized HO non-linear energy operators [50] or multi-dimensional TK energy operators [18];
2. The ESA, given by relations (6) and (7) [5,15,16,18,21,50–52], and ESA-based tools such as Teager-Huang transform [51] or Teager-Huang-Hough transform [40] work under positivity assumption;
3. Cross version of $\Psi_c(.)$ requires the positivity for its exploitation as a similarity measure for signals classification or time-delay estimation [53–58].

We show in this work that even in absence of noise and also for continuous version of the operator, this last can go negative, a situation that clearly undermines its physical significance as an energy operator. A more detailed analysis of the positivity conditions of $\Psi_c(.)$ is carried out, which extends and generalizes the findings reported in [48] and [47]. Unlike studies in [22,47,48] and [49], the new established positivity conditions are illustrated on both synthetic and real AM-FM signals.

1.1. Main contributions

1. The positivity problem of the TK energy operator is formulated logarithmically in terms of attenuation and phase, rather than the more conventional AM-FM model, which is equivalent to a geometrical interpretation of the positivity of $\Psi_c(.)$.
2. We show that the proposed formulation brings out the dependence of the positivity of $\Psi_c(.)$ on the initial phase of the input signal. To best of our knowledge the question of dependence of $\Psi_c(.)$ on the initial phase of the input signal has never been raised in the literature.
3. We highlight the existence of a critical interval over which the positivity of $\Psi_c(.)$ is depending on the initial phase of the input signal.
4. Results of this work extend and generalize the findings reported in [47] and [48].

1.2. Organization (outline)

In Section 2, we present the logarithmic formulation of positivity problem of the operator, which plays a key role in the proof of the reported results, followed by Theorem 1 that establishes sufficient condition of positivity, **CS1**, of $\Psi_c(.)$. We point out the geometrical interpretation of the positivity of the operator. Two normalized versions of **CS1** are summarized in **Corollary 1.1** (**CS2**), and **Corollary 1.2** (**CS3**). Condition **CS2** highlights that the positivity region is bounded by a parabola, while **CS3** states that this region is delimited by an hyperbola. In Section 3, we provide the positivity condition of the operator, excited by an AM-FM signal, termed as quadratic signal, whose attenuation and phase are of quadratic form: $\rho(t) = \rho_0 + \rho_1 t + \rho_2 t^2$; $\phi(t) = \phi_0 + \phi_1 t + \phi_2 t^2$. We prove the existence of critical interval over which the positivity of the operator is depending on the initial phase of the input signal. We show that the positivity analysis can be formulated as a geometric problem, and we give the proof of Theorem 2 that guarantees the positivity and highlights an interesting geometric meaning of the positivity. We next introduce Theorem 3 that gives the critical interval outside which the positivity of $\Psi_c(.)$ is guaranteed and there exists initial phase values for which $\Psi_c(.)$ is negative over this interval. We also state and prove **Corollary 3.1** that gives a time critical value from which $\Psi_c(.)$ is positive, and **Corollary 3.2** that underlines the fact that under condition **CS3**, if ϕ_1 and ϕ_2 have the same sign $\Psi_c(.)$ is positive for all $t \in \mathbb{R}^+$. We show that an AM-FM signal with $\rho(t)$ and $\phi(t)$ expanded in Taylor series of second order is also a quadratic signal, and thus condition **CS3** holds. We present Proposition 2 that proves that $\Psi_c(.)$ is positive for a linear chirp signal defined over $\mathbb{R}^+$. Results on simulated linear chirp signal and real bat echolocation signal are presented and the positivity of the operator analyzed in Section 4. We illustrate the dependence of the positivity of the operator by analyzing

different initial phase values of the input signal. More precisely, we identify the critical interval over which the positivity depends upon on the initial phase of the signal. We conclude the paper and discuss possible future work in Section 5.

2. AM-FM model

2.1. General condition & Logarithmic formulation

AM-FM signals are used to model a wide range of physical and biological phenomena (marine mammals, speech, biomedical signals, textured images,...) as well as in information transmission systems such as Radar and Sonar [11]. Thus, the positivity conditions analysis of $\Psi_c(.)$ is focused on this class of signals. In this work, the positivity problem is formulated logarithmically in terms of attenuation and phase of the input signal, rather than the more conventional AM-FM model. We illustrate the separate constraints upon amplitude modulation and phase as a subtle interplay. Our aim is to develop the initial work of Bovik and Maragos [47] and show that their log-concavity signal condition implies an interrelation between amplitude and phase of the input signal [48]. The log-concavity implies that an attenuation representation may be advantageous. Thus, we take the logarithm of the IA of the input signal $x(t)$ as follows:

$$\log\big(a(t)\big) = \rho(t) \;\Rightarrow\; x(t) = e^{\rho(t)}\cos\big(\phi(t)\big) \tag{9}$$

This model (Eq. 9) plays a key role in the proof of the results. Based on this model, we prove Theorem 1 which establishes the sufficient condition of positivity, **CS1**, of $\Psi_c(.)$. Positivity condition for the operator is simply $\Psi_c\big(s(t)\big) > 0$.

Theorem 1. *Operator $\Psi_c\big(x(t)\big)$ is strictly positive for any $t \in \mathbb{R}$ for which condition **CS1** holds :*

CS1: $\dot\phi^2(t) > \frac{1}{2}\Big(\ddot\rho(t) + \sqrt{\ddot\phi^2(t) + \ddot\rho^2(t)}\Big)$.

Proof. First and second derivatives of $x(t)$ are given by :

$$\dot x(t) = e^{\rho(t)}\big[\dot\rho(t)\cos\big(\phi(t)\big) - \dot\phi(t)\sin\big(\phi(t)\big)\big] \tag{10}$$

$$\begin{aligned}\ddot x(t) = e^{\rho(t)}\big[&(\ddot\rho(t) + \dot\rho^2(t) - \dot\phi^2)\cos\big(\phi(t)\big) - (2\dot\rho(t)\dot\phi(t)\\ &+ \ddot\phi(t))\sin\big(\phi(t)\big)\big]\end{aligned} \tag{11}$$

After simplification we get

$$\begin{aligned}\dot x(t)^2 - x(t)\ddot x(t) = e^{2\rho(t)}\big[&\dot\phi^2(t) + \ddot\phi(t)\sin\big(\phi(t)\big)\cos\big(\phi(t)\big)\\ &- \ddot\rho(t)\cos^2\big(\phi(t)\big)\big]\end{aligned} \tag{12}$$

Then, it follows that

$$\Psi_c(x(t)) = e^{2\rho(t)}g(t) \tag{13}$$

where function $g(t)$ is given by

$$g(t) = \dot\phi^2(t) + \ddot\phi(t)\sin\big(\phi(t)\big)\cos\big(\phi(t)\big) - \ddot\rho(t)\cos^2\big(\phi(t)\big) \tag{14}$$

Positivity of the first factor is guaranteed. Thus, the positivity of $\Psi_c(.)$ is reduced to the study of that of $g(t)$. Provided that $\ddot\rho(t)$ and $\ddot\phi(t)$ are not both simultaneously nulls, we get

$$\begin{aligned}g(t) = \dot\phi^2(t) - \frac{\ddot\rho(t)}{2} + \frac{\sqrt{\ddot\phi^2(t) + \ddot\rho^2(t)}}{2}\Big(&\frac{\ddot\phi(t)}{\sqrt{\ddot\phi^2(t) + \ddot\rho^2(t)}} \times \sin\big(2\phi(t)\big)\\ &- \frac{\ddot\rho(t)}{\sqrt{\ddot\phi^2(t) + \ddot\rho^2(t)}}\cos\big(2\phi(t)\big)\Big)\end{aligned} \tag{15}$$

There is a unique phase $\psi(t) \in]-\pi, \pi]$ such that

$$\cos(\psi(t)) = \frac{\ddot\phi(t)}{\sqrt{\ddot\phi^2(t) + \ddot\rho^2(t)}},\ \sin(\psi(t)) = \frac{\ddot\rho(t)}{\sqrt{\ddot\phi^2(t) + \ddot\rho^2(t)}} \tag{16}$$

Using trigonometric relation $\sin(a-b) = \sin(a)\cos(b) - \cos(a)\sin(b)$, the function $g(t)$ can therefore be rewritten as

$$g(t) = \Big(\dot\phi^2(t) - \frac{\ddot\rho(t)}{2}\Big) + \frac{\sqrt{\ddot\phi^2(t) + \ddot\rho^2(t)}}{2}\sin\big(2\phi(t) - \psi(t)\big) \tag{17}$$

Consequently, $g(t)$ is positive if

$$\dot\phi^2(t) - \frac{\ddot\rho(t)}{2} > \frac{\sqrt{\ddot\phi^2(t) + \ddot\rho^2(t)}}{2} \tag{18}$$

which complete the proof. □

Comment: Theorem 1 establishes the sufficient condition of positivity, **CS1**, of $\Psi_c(.)$. Formulated logarithmically in terms of attenuation $\rho(t)$ and phase $\phi(t)$, rather than the conventional AM-FM model, this theorem states that the positivity problem is limited to the positivity of only one function, $g(t)$. Interestingly, it highlights that the positivity depends neither on the attenuation $\rho(t)$ nor on its first order derivative $\dot\rho(t)$. Also, this theorem allows a geometric interpretation of the positivity of the operator. Indeed, we show in the following that normalizing relation (18) by $\dot\phi^2(t)$ or by $\ddot\phi(t)$ leads to a new formulation of condition **CS1**, and thus reducing the number of parameters. Normalization by $\dot\phi^2(t)$ leads to a positivity region bounded by a parabola [48]. By Theorem 1 we derive directly this parabolic positivity condition reported in [48]. Although limited to a restrictive class of signals, normalization by $|\ddot\phi(t)|$ allows a particular geometric approach, we will study next.

2.2. Normalization by $\dot\phi^2(t)$

Form of function $g(t)$ suggests that the number of variables can be reduced by defining normalized curvatures $\alpha(t)$ and $\beta(t)$ analogues to normalized chirp rates [48]:

$$\alpha(t) = \frac{\ddot\rho(t)}{\dot\phi^2(t)} \text{ and } \beta(t) = \frac{\ddot\phi(t)}{\dot\phi^2(t)} \tag{19}$$

Result of this normalization is stated by **Corollary 1.1**.

Corollary 1.1. *If $\dot\phi(t) \neq 0$, **CS1** is equivalent to condition*

CS2 : $|\beta(t)| < 2\sqrt{1-\alpha(t)}$

Proof. Dividing the two members of **CS1** by $\dot\phi^2(t)$ we get

$$2 - \alpha(t) > \sqrt{\alpha^2(t) + \beta^2(t)} \tag{20}$$

This inequality is equivalent to

$$\begin{cases}\big(2-\alpha(t)\big)^2 & > \alpha^2(t) + \beta^2(t)\\ \alpha(t) & > 2\end{cases} \tag{21}$$

which simplifies to $1 - \alpha(t) > \Big(\frac{\beta(t)}{2}\Big)^2$ and, so, complete the proof. □

Comment:

Corollary 1.1 also highlights that the positivity region is bounded by a parabola. Conditions **CS1** and **CS2** have been established by the upper bound $\big|\sin\big(2\phi(t) - \psi(t)\big)\big| \leqslant 1$. Study of parabolic condition **CS2** is detailed in [48]. In order to go further, let us keep the phase dependence of the sine term by avoiding this upper bound. Then, an hyperbolic condition is stated by Proposition 1.

Proposition 1. *Regions of positivity of $\Psi_c(.)$ are delimited by a family of hyperbolas, indexed by $\theta(t)$, and given by*

$$\alpha_1^2(t) - \beta^2(t) = 4\big(1 + \tau^2(t)\big) \tag{22}$$

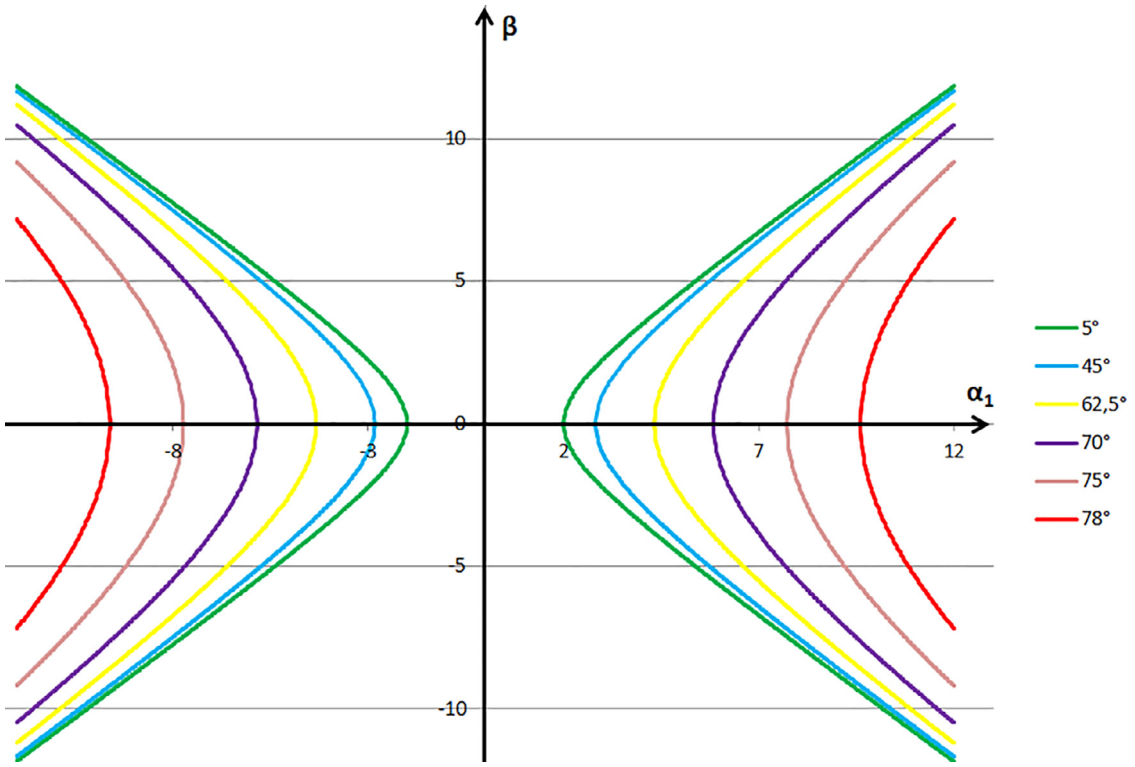

Fig. 1. Dependence of hyperbola curves upon the phase of the input signal.

where $\theta(t) = 2\phi(t) - \psi(t)$, $\tau(t) = \tan\big(\theta(t)\big)$ *and* $\alpha_1(t) = \dfrac{\alpha(t) - 2\big(1+\tau^2(t)\big)}{\tau(t)}$

Proof. Plugging $\alpha(t)$, $\beta(t)$ and $\theta(t)$ into relation (17), we get

$$g(t) = \frac{\dot{\phi}^2(t)}{2} v\big(\alpha(t), \beta(t), \theta(t)\big) \tag{23}$$

with

$$v\big(\alpha(t), \beta(t), \theta(t)\big) = \Big[2 - \alpha(t) + \sqrt{\alpha^2(t) + \beta^2(t)}\sin\big(\theta(t)\big)\Big] \tag{24}$$

To prove the positivity of $g(t)$, it is enough to prove the positivity of $v(t)$ given by the following inequality

$$\sqrt{\alpha^2(t) + \beta^2(t)}\sin\big(\theta(t)\big) \geqslant \alpha(t) - 2 \tag{25}$$

For a given $\theta(t)$ we obtain a region of $\mathbb{R}^2$ where the condition holds for the couples $\big(\alpha(t), \beta(t)\big)$, and the boundary of this region verifies the equality

$$(\alpha^2(t) + \beta^2(t))\sin^2\big(\theta(t)\big) = \big(2 - \alpha(t)\big)^2 \tag{26}$$

If $\theta(t) \neq 2k\pi$, $k \in \mathbb{Z}$, by setting $\tau(t) = \tan\big(\theta(t)\big)$, this equality is equivalent to

$$\left(\frac{\alpha(t) - 2\big(1+\tau^2(t)\big)}{\tau(t)}\right)^2 - \beta^2(t) = 4\big(1+\tau^2(t)\big) \tag{27}$$

which is the equation of an hyperbola. The change of coordinates system obtained by setting

$$\alpha_1(t) = \frac{\alpha(t) - 2\big(1+\tau^2(t)\big)}{\tau(t)} \tag{28}$$

leads to the proposition. Note that the case $\tau(t) = 0$, omitted above, is trivial. The positivity condition is simply $\alpha(t) < 2$.

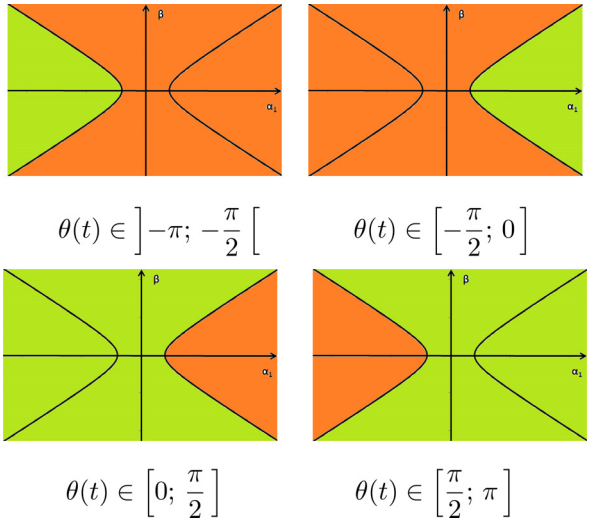

Fig. 2. Four positivity regions showing the dependence of the output of $\mathbf{\Psi}_c(x(t))$ on function $\theta(t)$.

The family of hyperbolas is depicted in Fig. 1. Regions of positivity of $\mathbf{\Psi}_c(.)$ are colored in green in Fig. 2. Once the curve limit is fixed, regions of positivity depend on $\theta(t)$. Different cases of positivity regions are represented in Fig. 2. □

2.3. Normalization by $\big|\ddot{\phi}(t)\big|$

Before dividing by $\big|\ddot{\phi}(t)\big|$, we have to consider the case $\big|\ddot{\phi}(t)\big| = 0$ which corresponds to a linear phase: $\phi(t) = \phi_0 + \phi_1 t$. Inserting $\phi(t)$ into relation (14), we get

$$g(t) = \phi_1^2 - \ddot{\rho}(t)\cos^2(\phi_0 + \phi_1 t) \tag{29}$$

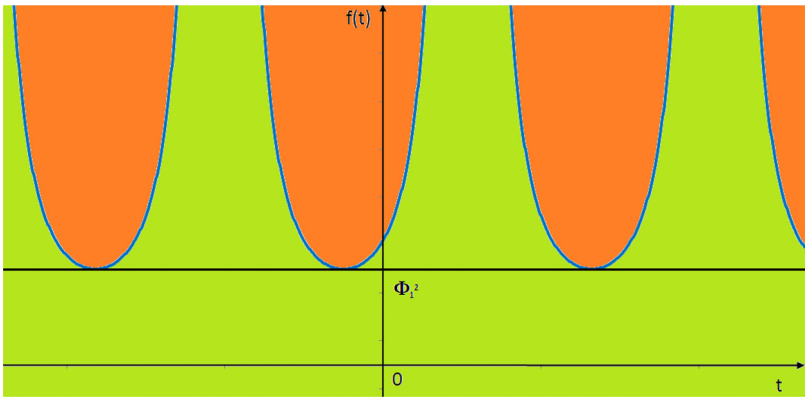

Fig. 3. Positivity region of linear phase signal delimited by curves of $f(t)$ is colored in green.

So, $g(t)$ is positive if and only if

$$\ddot{\rho}(t) < \frac{\phi_1^2}{\cos^2(\phi_0+\phi_1 t)} \tag{30}$$

where the second member of the inequality can possibly be $+\infty$. Thus, the positivity holds if $\ddot{\rho}(t) < \phi_1^2(t)$ and, more precisely if and only if $\ddot{\rho}(t) < f(t)$ where $f(t)$ is given by

$$f(t) = \frac{\phi_1^2}{\cos^2(\phi_0+\phi_1 t)} \tag{31}$$

The positivity condition is illustrated in Fig. 3, where $\mathbf{\Psi}_c(x(t))$ is positive in the half plane $\ddot{\rho}(t) < \phi_1^2$ and if, $\ddot{\rho}(t) > \phi_1^2$, outside the regions delimited by $f(t)$.

We now assume that $\ddot{\phi}(t) \neq 0$, except for a finite number of values of t. Result of the normalization is given by **Corollary 1.2**.

Corollary 1.2. *If $\ddot{\phi}(t) \neq 0$, condition **CS1** is equivalent to condition **CS3** :$\mu(t) > h\big(\lambda(t)\big)$,*

where $h\big(\lambda(t)\big) = \frac{1}{2}\Big(\lambda(t) + \sqrt{1+\lambda^2(t)}\Big)$, $\lambda(t) = \dfrac{\dddot{\rho}(t)}{|\ddot{\phi}(t)|}$ *and* $\mu(t) = \dfrac{\dot{\phi}^2(t)}{|\ddot{\phi}(t)|}$,

Proof. Simply divide two members of relation (18) by $|\ddot{\phi}(t)|$. □

Interpretation: Positivity of $\mathbf{\Psi_c}(.)$ is reduced to a relationship between two ratios

$$\lambda(t) = \frac{\dddot{\rho}(t)}{|\ddot{\phi}(t)|} \text{ and } \mu(t) = \frac{\dot{\phi}^2(t)}{|\ddot{\phi}(t)|} \tag{32}$$

Condition **CS3** ensures the positivity of $\mathbf{\Psi_c}(.)$ outside the hatched area as illustrated by Fig. 4.

Comment: Condition **CS3** can be simplified according to the magnitude order of $\lambda(t)$:

1. $\lambda(t) \sim 0 \Rightarrow h(\lambda(t)) \sim \frac{1}{2}\big(1+\lambda(t)\big)$
2. $\lambda(t) >> 1 \Rightarrow h(\lambda(t)) = \frac{\lambda(t)}{2}\Big(1+\sqrt{1+\frac{1}{\lambda^2(t)}}\Big) \sim \lambda(t)$
3. $\lambda(t) << -1 \Rightarrow h(\lambda(t)) = \frac{\lambda(t)}{2}\Big(1-\sqrt{1+\frac{1}{\lambda^2(t)}}\Big) \sim -\frac{1}{4\lambda(t)}$

Case $\lambda(t) >> 1$ leads to sufficient condition of positivity:

$$\dot{\phi}^2(t) > \ddot{\rho}(t) >> \left|\ddot{\phi}(t)\right| \tag{33}$$

In what follows we provide the positivity condition when $\mathbf{\Psi_c}(.)$ is excited by an AM-FM signal whose exponential attenuation and phase are of quadratic form. We prove the existence of critical interval over which positivity of $\mathbf{\Psi_c}(.)$ is depending on the initial phase of the input signal. To this end, we show that the positivity problem can be formulated as a geometric one.

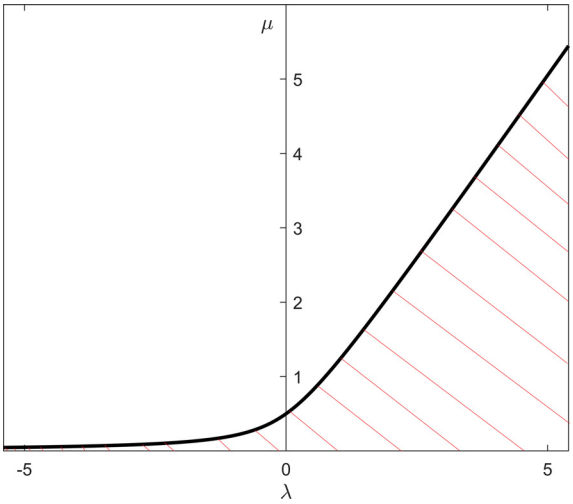

Fig. 4. Condition **CS3**.

3. Quadratic case

Consider an AM-FM signal where the attenuation and the phase are polynomial of degree 2:

$$\rho(t) = \rho_0 + \rho_1 t + \rho_2 t^2,\ \phi(t) = \phi_0 + \phi_1 t + \phi_2 t^2 \tag{34}$$

We term this case, quadratic signal. This can be derived locally by a development of $\rho(t)$ and $\phi(t)$ around a given instant t_0.

3.1. Geometric formulation of positivity

Theorem 2. *When a signal $x(t)$ is quadratic, the positivity of $\mathbf{\Psi_c}\big(x(t)\big)$ that holds on a $\mathscr{D}_t \subset \mathbb{R}$ domain is equivalent to the inequality*

$$(au+b) - k\sin(\Omega u + \varphi) > 0 \text{ on a domain } \mathscr{D}_u \subset \mathbb{R}^+ \tag{35}$$

where a, k and Ω are positive.

Proof. Since $x(t)$ is quadratic, relation (17) becomes

$$g(t) = \big(\dot{\phi}^2(t) - \rho_2\big) + \sqrt{\phi_2^2+\rho_2^2}\,\sin\big(2\phi(t) - \psi\big) \tag{36}$$

where $\psi = \psi(\rho_2, \phi_2) = \text{constant}$. Let us apply the non bijective parameter change $u = (t-d)^2$ with $d = -\phi_1/2\phi_2$. If $t \in I_t = [T_0;\ T_F] \subset \mathbb{R}$, then $u \in I_u = [u_0;\ u_F] \subset \overline{\mathbb{R}^+}$, where

1. if $d \notin I_t$: $u_0 = \inf\big\{(T_0-d)^2;\ (T_F-d)^2\big\}$ and $u_F = \sup\big\{(T_0-d)^2;\ (T_F-d)^2\big\}$;

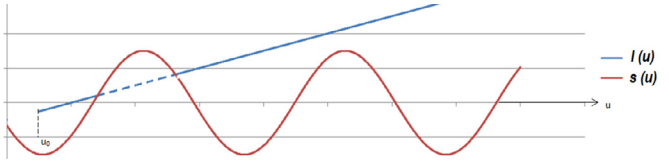

Fig. 5. Geometric interpretation of the positivity of $\Psi_c(.)$, excited by a quadratic signal.

2. if $d \in I_t$: u_0=0 and u_F=sup $\{(T_0-d)^2;\ (T_F-d)^2\}$.

Since $\phi(u)=\phi_2 u+\phi_0-\phi_2 d^2$ and

$$\dot{\phi}^2(u)=\left(\frac{\mathrm{d}\phi}{\mathrm{d}t}\right)^2(u)=4\phi_2^2 u \tag{37}$$

it follows that

$$g(u)=\left(4\phi_2^2 u-\rho_2\right)+\sqrt{\phi_2^2+\rho_2^2}\,\sin(2\phi_2 u+2\phi_0-2\phi_2 d^2-\psi) \tag{38}$$

By shifting the phase, we guarantee the positivity of u, in the sine function, and then it follows that:

$$g(u)=(au+b)-k\sin(\Omega u+\varphi) \tag{39}$$

where $u>0$, $\Omega=2|\phi_2|>0$, $a=4\phi_2^2=\Omega^2>0$, $b=-\rho_2$, $k=\sqrt{\phi_2^2+\rho_2^2}>0$ and

$$\varphi=\begin{cases}\pi-\arcsin\left(\dfrac{\rho_2}{k}\right)+(2\phi_0-2\phi_2 d^2) & \text{if } \phi_2\geqslant 0\\ \pi-\arcsin\left(\dfrac{\rho_2}{k}\right)-(2\phi_0-2\phi_2 d^2) & \text{if } \phi_2<0\,.\end{cases} \tag{40}$$

□

Geometric interpretation : Phase shifting makes the new form of $g(u)$ (Eq. 39) more amenable to check the positivity of $\Psi_c(.)$ by studying the sign of the difference between two functions namely, an affine function $l(u)=au+b$ and a sinusoidal function $s(u)=k\sin(\Omega u+\varphi)$. Resolving $(au+b)-k\sin(\Omega u+\varphi)>0$ on a domain $\mathscr{D}_u\subset\mathbb{R}^+$ then returns, from a geometric point of view, to determine the values of u for which the half-line (or segment) of equation $l(u)$ is above the sinusoid $s(u)$. The geometric meaning of the positivity of $\Psi_c(.)$ is illustrated in Fig. 5.

3.2. Critical interval and initial phase

Theorem 3. *When the signal $x(t)$ is quadratic (1) $\Psi_c(x(t))>0$ outside a time interval $I_c=[\,d-\gamma, d+\gamma\,]$;*

(2) if $t\in I_c$ there exist values of the initial phase ϕ_0 for which $\Psi_c(x(t))<0$;

where γ and λ_q are given by

$$\gamma=\frac{1}{2\sqrt{|\phi_2|}}\sqrt{\lambda_q+\sqrt{1+\lambda_q^2}}\ \text{ and }\ \lambda_q=\frac{\rho_2}{|\phi_2|} \tag{41}$$

Proof (1) : Since $s(u)\in[-k;\,k]$, therefore $g(u)$ will be positive when $l(u)>k$. Expressed as a function of t, this condition is written as

$$4\phi_2^2(t-d)^2-\rho_2>\sqrt{\phi_2^2+\rho_2^2} \tag{42}$$

or

$$|t-d|>\frac{1}{2|\phi_2|}\sqrt{\rho_2+\sqrt{\phi_2^2+\rho_2^2}} \tag{43}$$

Setting $d=-\dfrac{\phi_1}{2\phi_2}$ and using γ and λ_q, we obtain the condition $|t-d|>\gamma$, which means that $t\notin I_c$.

Proof (2) : Given the expression of φ (Eq. (39)), when the initial phase $\phi_0\in\mathbb{R}$, $\varphi\in[-\pi;\,\pi]$ and therefore, $s(t)=k\sin(\Omega t+\varphi)\in[-k;\,k]$. Additionally, if $I=I_t\bigcap[d-\gamma,\,d+\gamma]\neq\varnothing$, for $T\in I$, we have $u=(t-d)^2$ and $l(u)<k$. Then, there exits an initial phase value ϕ_0 for which $s(u)>l(u)$ and, therefore, $g(u)<0$.

Comment: Such a value of ϕ_0 is not unique. If $[T_0\,;T_F]\bigcap[d-\gamma,\,d+\gamma]\neq\varnothing$, there is a non-empty interval of values of ϕ_0 over which $\Psi_c(x(t))<0$. This interval is reduced to a singleton only in the individual cases where $T_F=d-\gamma$ or $T_0=d+\gamma$.

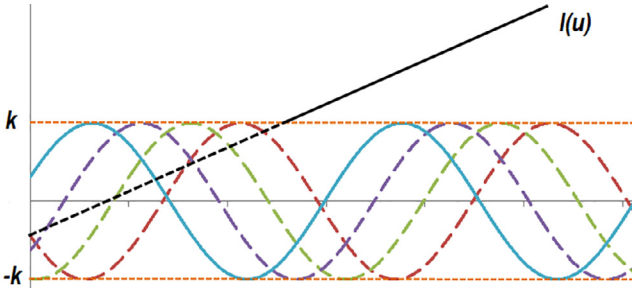

Fig. 6. Critical interval of the positivity of $\Psi_c(.)$.

Interpretation: The part of the half-line represented in Fig. 6 in dashed lines corresponds to an interval of values of t, critical interval, over which there are initial phases of the input signal making $\Psi_c(.)$ negative. Outside this range, the positivity of $\Psi_c(.)$ is guaranteed.

Corollary 3.1. *For a quadratic signal $x(t)$, there is a critical value τ_c from which $\Psi_c(x(t))$ is positive for all $t>\tau_c$.*

Proof. If $t>d+\gamma$, we have $\Psi_c(x(t))>0$ then, starting from $\tau_c=d+\gamma$, $\Psi_c(x(t))\geqslant 0$ and, for $t>\tau_c$, $\Psi_c(x(t))>0$. □

Corollary 3.2. *For a quadratic signal $x(t)$, if ϕ_1 and ϕ_2 have the same sign and condition **CS3b** holds, then $\Psi_c(x(t))>0\ \forall t\in\mathbb{R}^+$:*

***CS3b** : $\mu_q>h(\lambda_q)$*

where

$$\mu_q=\frac{\phi_1^2}{2|\phi_2|},\ \lambda_q=\frac{\rho_2}{|\phi_2|}\ \text{and}\ h(\lambda_q)=\frac{1}{2}\left(\lambda_q+\sqrt{1+\lambda_q^2}\right)$$

Proof. By **Corollary 3.1**, if $\tau_c<0$, thus $\Psi_c(x(t))>0$ for $t\in\,]\,\tau_c\,;+\infty]$ with $\mathbb{R}^+\subset\,]\,\tau_c\,;+\infty]$. Since γ is always positive, $\tau_c<0$ is equivalent to the two simultaneous conditions $d<0$ and $d^2>\gamma^2$. On the one hand d is negative if, and only if, ϕ_1 and ϕ_2 are of the same sign, on the other hand the inequality $d^2<\gamma^2$ is equivalent to

$$\frac{\phi_1^2}{4\phi_2^2}>\frac{1}{4|\phi_2|}\left(\lambda_q+\sqrt{1+\lambda_q^2}\right) \tag{44}$$

where $\lambda_q=\dfrac{\rho_2}{|\phi_2|}$. Note $\mu_q=\dfrac{\phi_1^2}{2|\phi_2^2|}$ to get the expected result. **Corollary 3.3** provides the positivity condition for $t_0=0$. □

Corollary 3.3. *For a quadratic signal $x(t)$, provided that **CS3** holds, then $\Psi_c(x(0))>0$.*

Proof. We must have $0\notin I_c$, which is the case, either if

1. $d+\gamma<0$ (case previously studied) which is verified if $d<0$ and if the condition **CS3b** holds, or if
2. $d-\gamma>0$ which needs in a similar way the realization of $d>0$ and **CS3**, whence the statement of the corollary.

We show in the following that, using a local quadratic model, condition **CS2** stated in the general AM-FM case is verified. □

3.3. Local quadratic model

Consider an AM-FM signal $x(t) = e^{\rho(t)} \cos\phi(t)$, with the attenuation and phase expanded in Taylor series of second order around $t = t_0$:

$$\phi(t) \simeq \phi(t_0) + (t - t_0)\dot{\phi}(t_0) + 0.5(t - t_0)^2\ddot{\phi}(t_0) \tag{45}$$

$$\rho(t) \simeq \rho(t_0) + (t - t_0)\dot{\rho}(t_0) + 0.5(t - t_0)^2\ddot{\rho}(t_0) \tag{46}$$

Setting $\phi_0 = \phi(t_0)$, $\phi_1 = \dot{\phi}(t_0)$, $\phi_2 = \frac{1}{2}\ddot{\phi}(t_0)$, $\rho_0 = \rho(t_0)$, $\rho_1 = \dot{\rho}(t_0)$ and $\rho_2 = \frac{1}{2}\ddot{\rho}(t_0)$, we get $x(t) \simeq x_q(t - t_0)$ where

$$\phi_q(t) = \rho_0 + \rho_1 t + \rho_2 t^2, \rho_q(t) = \phi_0 + \phi_1 t + \phi_2 t^2 \tag{47}$$

Thus,

$$x_q(t) = e^{\rho_q(t)} \cos\phi_q(t) \tag{48}$$

is a quadratic signal. Positivity of $\Psi_c\big(x(t)\big)$ at $t_0 \neq 0$ is thus reduced to that of $\Psi_c\big(x_q(t)\big)$ at $t_0 = 0$. The latter holds for $t_0 = 0$ does not belong to interval $I_c = [\, d - \gamma\,,\, d + \gamma\,]$, so, by **Corollary 3.2** condition **CS3** holds. Given parameters ρ_i and ϕ_i, $i \in \{0, 1, 2\}$, we get $\mu_q = \mu(t_0)$ and $\lambda_q = \lambda(t_0)$. We next prove that positivity (subsection 3.2) holds for a class of AM-FM signals namely, linear chirp signals.

3.4. Linear chirp

A signal $x(t) = a(t)\cos(\phi(t))$ is called chirp if the following conditions are checked [59]:

$$(\mathbf{C1}) : \left|\dot{a}(t)\,/\,a(t)\dot{\phi}(t)\right| << 1 \text{and } (\mathbf{C2}) : \left|\ddot{\phi}(t)\,/\,\dot{\phi}^2(t)\right| << \ 1\,.$$

Using $a(t) = e^{\rho(t)}$ these conditions can be rewritten as follows

$$(\mathbf{C11}) : \left|\dot{\rho}(t)\,/\,\dot{\phi}(t)\right| << 1 \text{and } (\mathbf{C21}) : \left|\ddot{\phi}(t)\,/\,\dot{\phi}^2(t)\right| << 1\,.$$

We will call $x(t)$ linear chirp if variations of $\rho(t)$ and $\phi(t)$ are linear, i.e. if $x(t)$ is, moreover, quadratic.

Proposition 2. *The operator $\Psi_c(.)$ is positive for a linear chirp signal defined on $\mathbb{R}^+$.*

Proof. For a quadratic signal, setting $d = -\dfrac{\phi_1}{2\phi_2}$, $m = -\dfrac{\rho_1}{2\rho_2}$ and $\lambda = \dfrac{\rho_2}{|\phi_2|}$, **C12** and **C22** can be written as

$$(\mathbf{C12}) : \left|\lambda\,\frac{t-m}{t-d}\right| << 1 \ \text{ and } \ (\mathbf{C22}) : \left|\frac{1}{2\phi_2(t-d)^2}\right| << 1$$

Condition **C22** cannot be satisfied on $\mathbb{R}$ because the first member tends to ∞ when t is close to d. Let's study this signal. We need to have $d < 0$ so **C22** holds on $\mathbb{R}^+$. Thus,

ϕ_1 and ρ_1 must have the same sign (R1).

When $t \to \infty$, condition **C12** imposes $|\lambda| << 1$ and, when $t \to 0$, condition **C22** imposes $\mu >> 1$. So we have

$$\mu >> h(\lambda) = \tfrac{1}{2}\left(\lambda + \sqrt{1 + \lambda^2}\right) \tag{R2}.$$

Given (R1) and (R2), conditions of **Corollary 3.3** hold and $\Psi_c(.)$ is positive. □

4. Results

We study the positivity of TK energy operator on both synthetic and real signals.

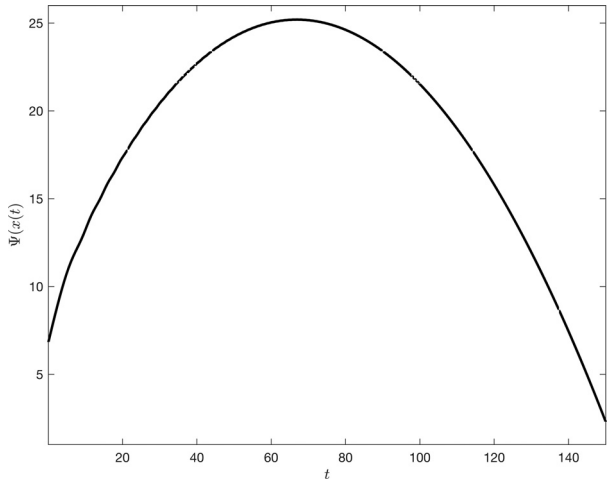

Fig. 7. $\Psi_c(x(t))$ of the linear chirp.

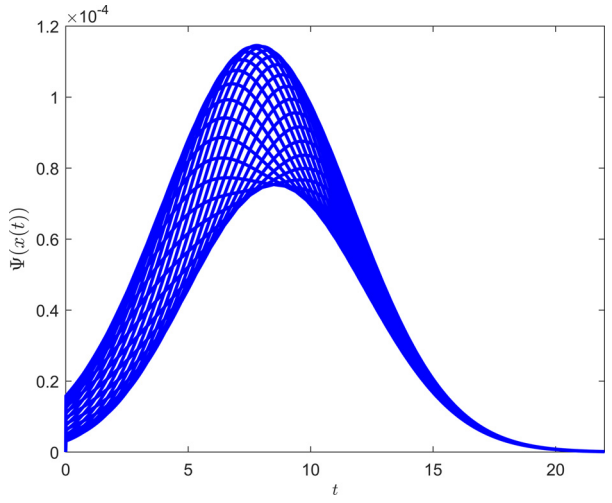

Fig. 8. Corollary 3.2 holds.

4.1. Linear chirp signal

We illustrate **Corollary 3.3** through a synthetic linear chirp signal given by

$$x(t) = e^{\rho(t)} \cos\big(\phi(t)\big) \tag{49}$$

where $\rho(t) = -4 + 0.2t + 0.0016t^2$ and $\phi(t) = 2 + 0.19t + 0.02t^2$. Figure (7) represents the output of $\Psi_c(x(t))$. For sake of visibility of the sign of $\Psi_c(x(t))$, a normalized version of $\Psi_c(.)$ is used:

$$z(t) = \ln\left(\frac{\kappa\,\Psi_c(x(t))}{\inf\left(\Psi_c\left(x(t)\right)\right)}\right) \tag{50}$$

where κ is set to 10. As expected, by **Corollary 3.3** the operator is positive.

For a quadratic AM-FM signal, sufficient condition of positivity of $\Psi_c(.)$ is verified. This condition proves, moreover, necessary for the positivity to be independent of the initial phase of $x(t)$. We report in Fig. 8 the output of $\Psi_c(.)$ for a quadratic signal $x(t)$, satisfying the criteria of **Corollary 3.2**, with the parameters: $\rho_0 = -4$, $\rho_1 = 0.2$, $\rho_2 = -0.0016$; $\phi_1 = 0.1$, $\phi_2 = 0.01$, $-\pi \leq \phi_0 \leq +\pi$. The operator remains positive on $\mathbb{R}^+$. Using the same parameters but with ϕ_2 set to -0.01, Fig. 9 shows that the criteria of **Corollary 3.2** are not checked, and this is expected because ϕ_1 and ϕ_2 have not the same sign. There are phase values for which $\Psi_c\big(x(t)\big)$ is

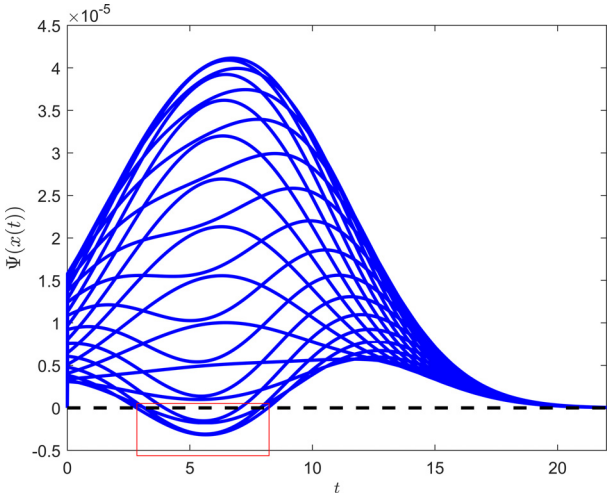

Fig. 9. Corollary 3.2 does not hold. The box indicating the critical interval.

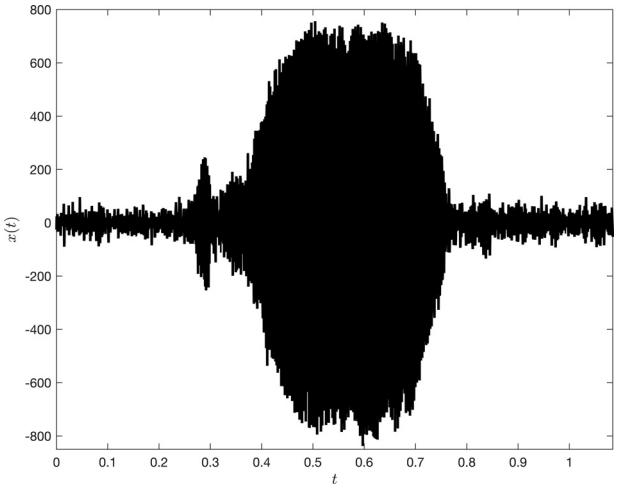

Fig. 10. Sonar signal from a bat.

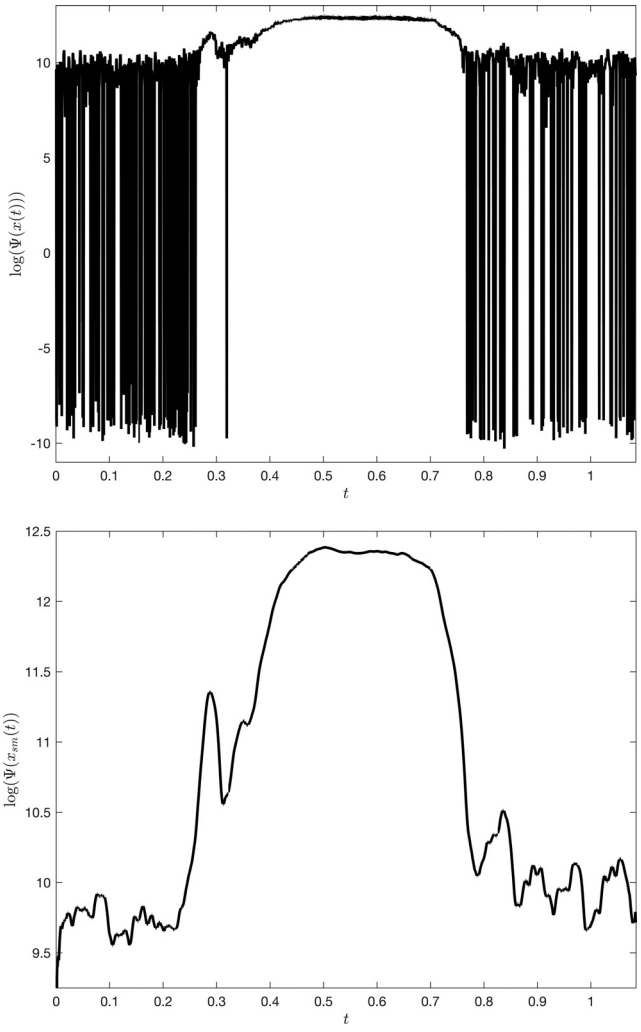

Fig. 11. Logarithmic scale representation of the output of the operator $\log \Psi(.)$, applied to real signal $x(t)$, and its smoothed version $x_{sm}(t)$.

negative in the critical interval $t \in [2.5, 7.5]$. Note that this interval is centered around the value $d = -\phi_1/2\phi_2 = 5$. To the best of our knowledge, this problem of sensitivity of $\mathbf{\Psi}_c(.)$ to initial phase of the input signal has never been pointed out or studied in the literature.

4.2. Application to real data

Positivity conditions of $\mathbf{\Psi}_c(.)$ have been established for continuous AM-FM signals. These conditions are checked on real bat echolocation signal (AM-FM signal), recorded with a sampling frequency of 230 kHz and an effective bandwidth of [8kHz, 80kHz].

The output $\mathbf{\Psi}_c(.)$ is calculated using its discrete version (Eq. 2). To highlight the positivity region of $\mathbf{\Psi}_c(.)$, a logarithmic scale representation is used

$$\log \Psi(.) = \text{sign}(\text{TK}_d) \log_{10}\left(1 + |\text{TK}_d|\right) \tag{51}$$

Fig. 11 depicts two time domains where $\log \Psi(.)$, applied to real signal $x(t)$, takes negative values. However, using a smoothed version of the signal, $x_{sm}(t)$, using a judicious filtering such as Savitsky-Golay filter [60,61], the output of the operator will be positive everywhere. To test the conditions of positivity, samples of the real signal are fitted by the AM-FM model given by relation (9) followed by its demodulation. For the real signal of bat, discrete version of ESA (DESA) is used [46]. To ensure the operator's non-negativity, the following criterion derived from condition **CS1** must be positive.

$$\text{CS}_1 = \dot{\phi}^2(t) - \frac{1}{2}\left(\ddot{\rho}(t) + \sqrt{\ddot{\phi}^2(t) + \ddot{\rho}^2(t)}\right) \tag{52}$$

To compute CS_1, the real signal is demodulated using DESA and the associated AM-FM signal (Eq. 9) reconstructed.

Fig. 12 shows that, compared to results reported in Fig. 11, $\mathbf{\Psi}_c(.)$ exhibits less negative values due to smoothing effect of the AM-FM modeling (Eq. 9). Criterion CS_1 evidences the instants where $\mathbf{\Psi}_c(.)$ is negative, but it seems to be less exploitable. Also, a careful examination of two plots of Fig. 12, shows that there is no apparent link between the positivity of CS_1 and the output of $\mathbf{\Psi}_c(.)$. These observations raise issues that need to be addressed. Indeed, these issues can be related to noise level that contaminates the signal, the sampling rate of the signal or to its initial phase. To understand these problems and provide solutions, the real signal is approximated with a convenient mathematical model.

Analytic model

We built an analytical model to gain an understanding of positivity conditions of $\mathbf{\Psi}_c(.)$ applied to real signal. We aim at constructing a continuous function that could represent the empirical law which is behind the finite set of data. To approximate this real

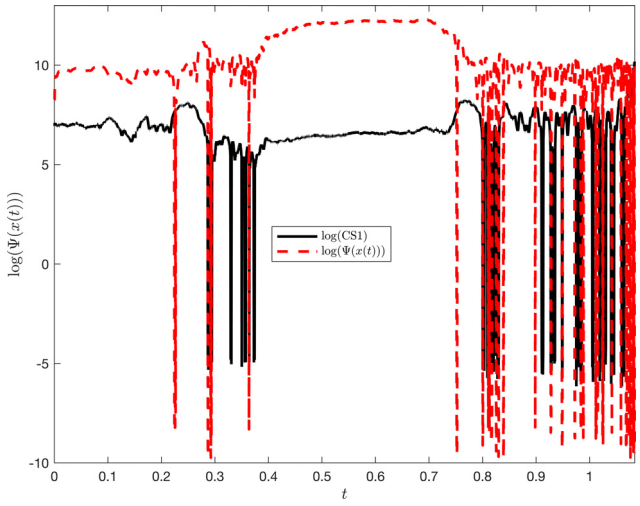

Fig. 12. Logarithmic scale representations of CS_1 and the output of the operator, applied to signal after demodulation by DESA.

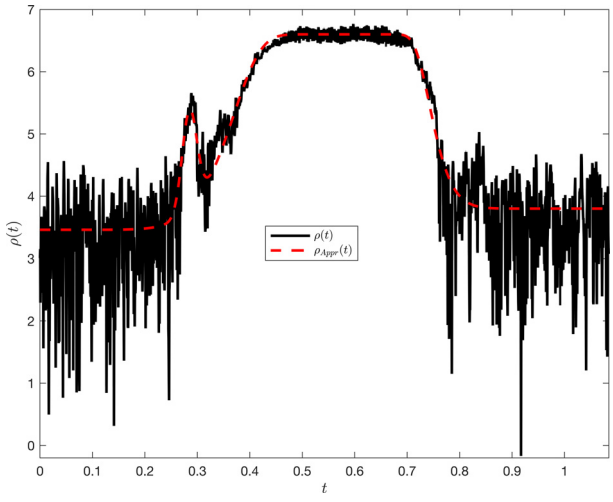

Fig. 13. Approximation of $\rho(t)$ using $f_i(t)$ functions.

signal, we model its modulating components $\rho(t)$ and $\omega(t)$ by the following functions

$$\rho(t) \simeq \rho_{Appr}(t) = f_1(t) + f_2(t) + f_3(t) \tag{53}$$

$$\omega(t) \simeq \omega_{Appr}(t) = g_1(t) + g_2(t) + g_3(t) + g_4(t) \tag{54}$$

Mathematical expressions of $f_i(t)$ and $g_k(t)$ and their derivatives with respect to time are detailed in appendix section. Approximations of $\rho(t)$ and $\omega(t)$ using respectively $f_i(t)(\rho_{Appr}(t))$ and $g_k(t)(\omega_{Appr}(t))$ functions are depicted in Figs. 13 and 14.

Fig. 15 shows that criterion CS_1, applied to signal approximated by the analytic model, takes negative values on two intervals, which are well evidenced on the zoomed plot of CS_1 over the interval [0.25, 0.35] (Fig. 16). Operator $\mathbf{\Psi}_c(.)$ takes negative values on the same intervals (Fig. 17), but not only as shown on the zoom of plot of $\mathbf{\Psi}_c(.)$ over the interval [0.25, 0.35] (Fig. 18). This can be explained by sampling rate. Using the constructed analytic model, both signal $x(t)$ and the output of $\mathbf{\Psi}_c(.)$ can be sampled at any rate. Thus, using a down-sampling by a factor 4, Fig. 19 shows that there are two intervals where the operator $\mathbf{\Psi}_c(.)$ takes negative values, but only in the second interval the positivity condition **CS1** is not respected. This result is expected since **CS1** is sufficient and not a necessary condition.

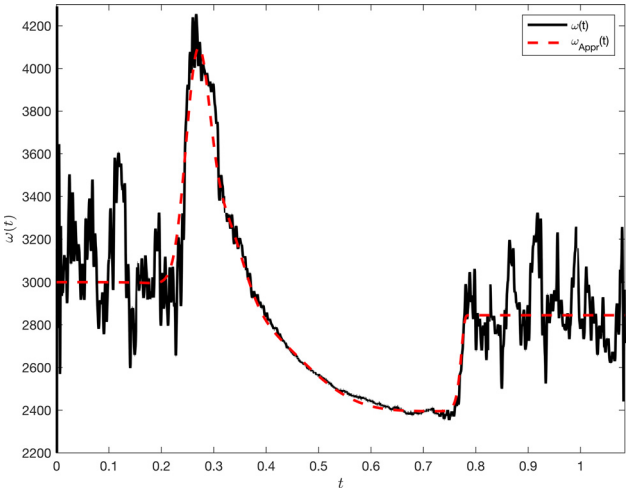

Fig. 14. Approximation of $\omega(t)$ using $g_k(t)$ functions.

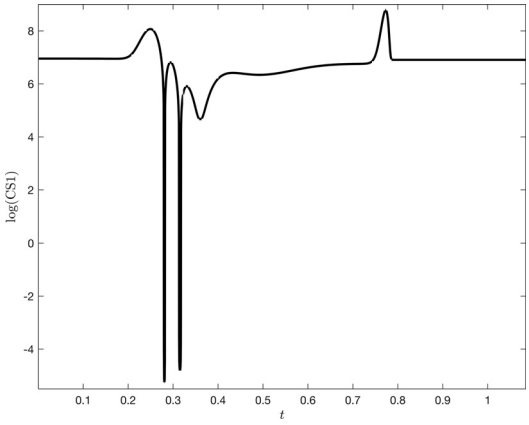

Fig. 15. Logarithmic scale representation of the positivity criterion CS_1 applied to signal approximated by the analytic model.

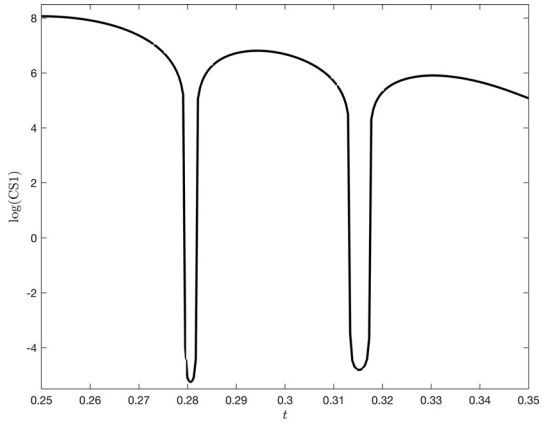

Fig. 16. Zoom over the interval [0.25, 0.35] of the plot of CS_1.

Dependence on the initial phase

The influence of the initial phase of the input signal must be taken into account. Experimentally, for a given time discretization step h this amounts to shifting samples with an amount less than h. Outputs of $\mathbf{\Psi}_c(.)$ depend upon the time alignment of the time discretization grid. As depicted in Fig. 20, by varying this grid, a family of curves corresponding to different initial phase values is obtained. These curves highlight the sensitivity of the operator's

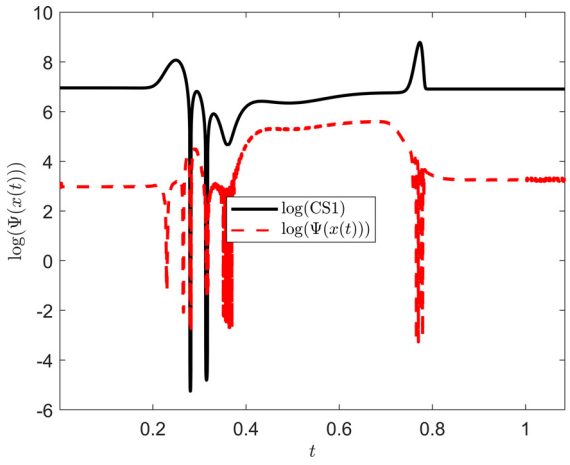

Fig. 17. Logarithmic scale representation of the positivity criterion CS_1 and the output of $\Psi_c(.)$ applied to signal approximated by the analytic model.

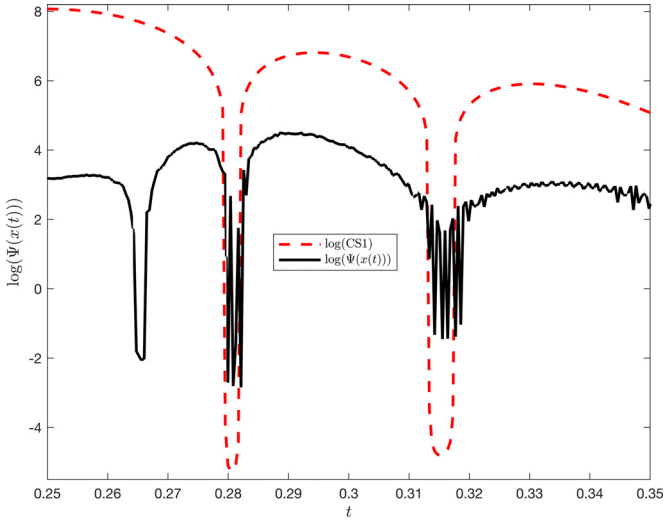

Fig. 18. Positivity criterion CS_1 versus operator over the interval [0.25, 0.35].

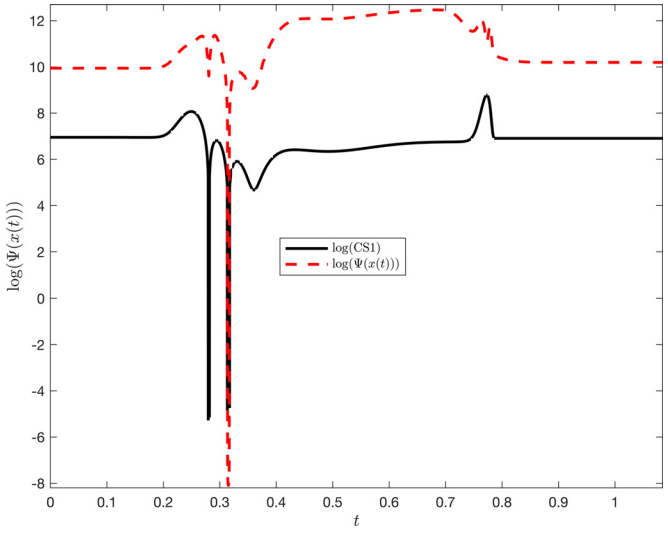

Fig. 19. Positivity criterion CS_1 versus $\Psi_c(.)$ using a down-sampling by a factor 4.

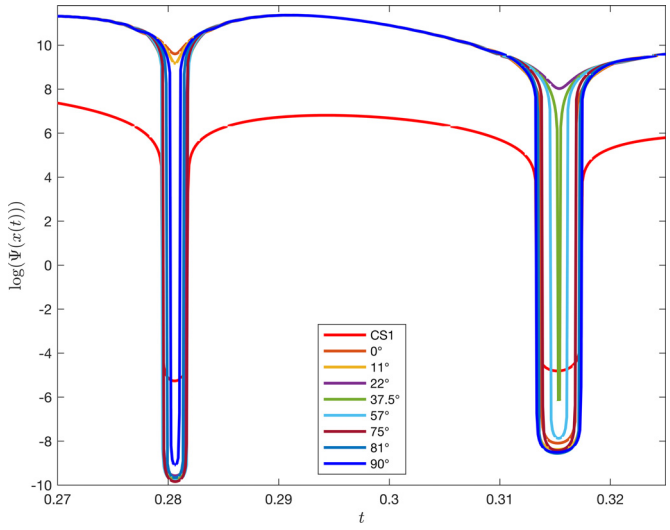

Fig. 20. Positivity criterion CS_1 versus operator for different initial phase values of the input signal.

output to the initial phase value of the input signal. Note that this sensitivity to initial phase manifests itself only on time intervals where the positivity criterion is not satisfied.

Comment: Unlike the method of Bovik and Maragos [47], our approach establishes the sufficient conditions of positivity of the operator for the class of AM-FM signals and brings out the dependence of the positivity on the initial phase of the input signal. More precisely, our approach highlights the existence of a critical interval over which the operator depends upon on the initial phase of this signal. Provided the analytic model of the signal, the proposed method allows to predict the positivity or the negativity of the operator, and this prediction cannot be done with the method of Bovik and Maragos. This why analysis of both synthetic and real signals have not been compared to this method, because it does not take into account initial phase information of the signals.

5. Conclusions

In this work, we have established, in the general case of AM-FM signals, a sufficient condition of positivity of the TK energy operator resulting in Theorem 1. This condition is equivalent, locally, to that of positivity in zero (**Corollary 3.3**) of the quadratic signal $x_q(t)$ obtained by a Taylor expansion of input signal $x(t)$. The local study allows us to better apprehend the conditions of positivity and will be the object of later developments as well as the discrete transposition of these conditions for a sampled signal. In the case of quadratic signal, the geometrical formulation brings out the dependence of the positivity of TK energy operator on the initial phase of the signal. Furthermore, we highlight the existence of a critical interval over which the positivity of the operator is depending on the initial phase. Outside this interval, the positivity is preserved. As future research, we plan to extend this work to large class of signals and particularly to images.

Declaration of Competing Interest

The Authors declare that there is no conflict of interest.

Acknowledgement

The authors thank the Associate Editor and the Reviewers for their gracious comments and helpful suggestions that have greatly improve the quality of the manuscrit. We appreciate the careful

reading of Reviewer #2. Also, the authors would like to thank Ecole Navale for its support.

Appendix

$$f_1(t) = C_{11}\left[1 - e^{-(A_1(t))^{k_1}}\right], f_2(t) = m_1 - C_{12}\, e^{-(A_2(t))^{k_2}}$$
$$f_3(t) = \frac{a_1}{s_1\sqrt{2\pi}}\, e^{-(B_1(t))^2}, g_1(t) = C_{33}\, e^{u_3(A_3(t))^{k_3}}$$
$$g_2(t) = C_{34}\left[1 - e^{u_4(A_4(t))^{k_4}}\right], g_3(t) = m_3 + \frac{a_3}{s_3\sqrt{2\pi}}\, e^{-(B_3(t))^2}$$
$$g_4(t) = \frac{a_4}{s_4\sqrt{2\pi}} e^{-(B_4(t))^2}$$

where $G_i = \frac{2a_i}{s_i^3\sqrt{2\pi}}$, $F_i = t - e_i$, $E_i = \frac{k_i}{\lambda_i}$, $C_{ij} = (M_i - m_j)$, $D_i = \frac{k_i - 1}{\lambda_i}$, $A_i(t) = \frac{t - t_i}{\lambda_i}$, $B_i(t) = \frac{t - e_i}{s_i}$, $M_1 = 6.6$, $m_1 = 3.46$, $m_2 = 3.8$, $t_1 = 0$, $\lambda_1 = 0.375$, $k_1 = 8$, $t_2 = 1.05$, $\lambda_2 = 0.31$, $k_2 = 12$, $a_1 = 0.08$, $s_1 = 0.02$, $e_1 = 0.285$, $M_3 = 3000$, $m_3 = 2395$, $m_4 = 2550$, $t_3 = 0$, $\lambda_3 = 0.5$, $k_3 = 5$, $u_3 = -1.3$, $t_4 = 0.073$, $\lambda_4 = 0.7$, $k_4 = 120$, $u_4 = -1$, $a_3 = 46$, $s_3 = 0.05$, $e_3 = 0.32$, $a_4 = 80$, $s_4 = 0.032$, $e_4 = 0.269$.

$\dot{\rho}(t) = \dot{f}_1(t) + \dot{f}_2(t) + \dot{f}_3(t)\dot{\omega}(t) = \dot{g}_1(t) + \dot{g}_2(t) + \dot{g}_3(t) + \dot{g}_4(t)\ddot{\rho}(t) = \ddot{f}_1(x) + \ddot{f}_2(x) + \ddot{f}_3(x)$ and $\ddot{\omega}(t) = g_1''(t) + g_2''(t) + \ddot{g}_3(t) + \dot{g}_4(t)$ where

$$\dot{f}_1(t) = C_{11}E_1(A_1(t))^{k_1-1}e^{-(A_1(t))^{k_1}}$$
$$\dot{f}_2(t) = C_{12}E_2(A_2(t))^{k_2-1}e^{-(A_2(t))^{k_2}}$$
$$\dot{f}_3(t) = -G_1(t - e_1)e^{-(B_1(t))^2},$$
$$\dot{g}_1(t) = C_{33}u_3E_3(A_3(t))^{k_3-1}e^{-(A_3(t))^{k_3}}$$
$$\dot{g}_2(t) = -C_{34}u_4E_4(A_4(t))^{k_4-1}e^{-(A_4(t))^{k_4}}$$
$$\dot{g}_3(t) = -G_3F_3e^{-(B_3(t))^2}, \dot{g}_4(t) = -\frac{2a_4}{s_3^3\sqrt{2\pi}}F_4e^{-(B_4(t))^2}$$
$$\ddot{f}_1(t) = C_{11}E_1\left[D_1(A_1(t))^{k_1-2} - E_1(A_1(t))^{2k_1-2}\right]e^{-(A_1(t))^{k_1}}$$
$$\ddot{f}_2(t) = C_{12}E_2\left[D_2(A_2(t))^{k_2-2} - E_2(A_2(t))^{2k_2-2}\right]e^{-(A_2(t))^{k_2}}$$
$$\ddot{f}_3(t) = \frac{2a_1}{s_1^3\sqrt{2\pi}}\left[\frac{2}{s_1^2}F_1^2 - 1\right]e^{-B_1(t)^2},$$
$$\ddot{g}_1(t) = C_{33}u_3E_3\left[D_3(A_3(t))^{k_3-2} + u_3E_3(A_3(t))^{2k_3-2}\right]e^{u_3(A_3(t))^{k_3}}$$
$$\ddot{g}_2(t) = -C_{34}u_4E_4\left[D_4(A_4(t))^{k_4-2} + u_4E_4(A_4(t))^{2k_4-2}\right]e^{u_4(A_4(t))^{k_4}}$$
$$\ddot{g}_3(t) = G_3\left[\frac{2}{s_3^2}F_3^2 - 1\right]e^{-(B_3(t))^2}, \ddot{g}_4(t) = G_4\left[\frac{2}{s_4^2}F_4^2 - 1\right]e^{-(B_4(t))^2}$$

$\phi(t) = \omega(t).t\dot{\phi}(t) = \dot{\omega}(t).t + \omega(t)$ and $\ddot{\phi}(t) = \ddot{\omega}(t).t + 2\dot{\omega}(t)$.

References

[1] H. M. Teager, private communication, 1985.
[2] H.M. Teager, S.M. Teager, Evidence for nonlinear sound production mechanisms in the vocal tract, Speech Production and Speech Modelling, NATO ASI Series 55 (1989) 241–261.
[3] J.F. Kaiser, On a simple algorithm to calculate the 'energy' of a signal, Proc. ICASSP, (1990) 381–384.
[4] J.F. Kaiser, On teager's energy algorithm and its generalization to continuous signals, Proc. IEEE DSP Workshop, (1990).
[5] P. Maragos, J.F. Kaiser, T.F. Quatieri, On amplitude and frequency demodulation using energy operators, IEEE TSP, 41 (4) (1993) 1532–1550.
[6] D. Vakman, On the analytic signal, the teager-kaiser energy algorithm, and other methods for defining amplitude and frequency, IEEE TSP, 44 (4) (1996) 791–797.
[7] D. Dimitriadis, A. Potamianos, P. Maragos, A comparison of the squared energy and teager-kaiser operators for short-term energy estimation in additive noise, IEEE TSP, 57 (7) (2009) 2569–2581.
[8] P.F. Pai, Instantaneous frequency of an arbitrary signal, International Journal of Mechanical Sciences, 52 (2010) 1682–1693.
[9] R.B. Randall, W.A. Smith, Uses and mis-uses of energy operators for machine diagnostics, Mechanical Systems and Signal Processing, 133 (2019) 1–20.
[10] B. Picinbono, On instantaneous amplitude and phase of signals, IEEE TSP, 45 (3) (1997) 552–560.
[11] J. Proakis, M. Salehi, Digital Communications, McGraw-Hill, 2007. 5th Ed.
[12] B.P. Lathi, Modern Digital and Analog Communication Systems, University Press, Oxford, 1998.
[13] S. Haykin, Communication Systems, 2nd Ed, New York, Wiley, 1983.
[14] P. Maragos, A.C. Bovik, Image demodulation using multidimensional energy separation, JOSA A, 12 (9) (1995) 1867–1876.
[15] A.O. Boudraa, F. Salzenstein, J.C. Cexus, Two-dimensional continuous higher-order energy operators, Opt. Eng., 44 (11) (2005) 7001–7010.
[16] E.H.S. Diop, A.O. Boudraa, F. Salzenstein, A joint 2d AM-FM estimation based on higher order teager-kaiser energy operators, Sig. Imag. Video Proc., 5 (1) (2011) 61–68.
[17] A. Bouchikhi, A.O. Boudraa, Multicomponent AM-FM signals analysis based on EMD-b-splines ESA, Sig. Proc., 92 (9) (2012) 2214–2228.
[18] F. Salzenstein, A.O. Boudraa, T. Chonavel, A new class of multi-dimensional teager-kaiser and higher order operators based on directional derivatives, Multidimens. Syst. Sig. Proc., 24 (2013) 543–572.
[19] F. Salzenstein, P. Montgomery, A.O. Boudraa, Local frequency and envelope estimation by teager-kaiser energy operators in white-light scanning interferometry, Optics Express, 22 (15) (2014).
[20] P. Maragos, A. Potamianos, Higher order differential energy operators, IEEE SPL, 2 (1995) 152–154.
[21] W. Liu, A. Santhanam, Wideband image demodulation via bi-dimensional multirate frequency transformations, JOSA A, 33 (9) (2016). 1678–1668
[22] P. Maragos, J.F. Kaiser, T.F. Quatieri, Energy separation in signal modulation with application to speech analysis, IEEE TSP, 41 (10) (1993) 3024–3051.
[23] G. Evangelopoulos, P. Maragos, Multiband modulation energy tracking for noisy speech detection, IEEE TASLP, 14 (6) (2006) 2024–2038.
[24] D. Dimitriadis, P. Maragos, A. Potamianos, On the effects of filterbank design and energy computation on robust speech recognition, IEEE TASLP, 19 (6) (2011) 1504–1516.
[25] K. Khaldi, A.O. Boudraa, A. Komaty, Speech enhancement using empirical mode decomposition and teager-kaiser energy operator, JASA, 135 (1) (2014) 451–459.
[26] N. Shokouhi, J.H.L. Hansen, Teager-kaiser energy operators for overlapped speech detection, IEEE TASLP, 25 (5) (2017) 1035–1047.
[27] S. Solnik, P. Rider, K. Steinweg, P. De Vita, T. Hortobagyi, Teager-kaiser energy operator signal improves EMG onset detection, Eur. J. Appl. Physiol. 110 (2010) 489–498.
[28] R. Thirumuru, A.K. Vuppala, Application of non-negative frequency-weighted energy operator for vowel region detection, Int. J. Speech Techno. 21 (2018) 279–291.
[29] M.R. Kamble, Detection of replay spoof speech using teager energy feature cues, Computer Speech & Language, 65 (2021) 1–19.
[30] S. Mukhopadhyay, G.C. Ray, A new interpretation of nonlinear energy operator and its efficacy in spike detection, IEEE TBE 45 (2) (1998) 180–187.
[31] X. Li, A.S. Aruin, Muscle activity onset time detection using teager-kaiser energy operator, Conf. IEEE EMBS (2005) 7549–7552.
[32] V. Kandia, Y. Stylianou, Detection of sperm whale clicks based on the teager-kaiser energy operator, Applied Acoustics 67 (11) (2006) 1144–1163.
[33] A.O. Boudraa, J.C. Cexus, K. Abed-Meraim, Cross-ψ_b-energy operator-based signal detection, JASA, 132 (6) (2008). 4283–4283
[34] A.O. Boudraa, J.C. Cexus, S. Benramdane, T. Chonavel, Some useful properties of cross-ψ_b-energy operator, Int. J. Elec. Comm. 63 (2009) 728–735.
[35] A. Drira, L. Guillon, A.O. Boudraa, Image source detection for geoacoustic inversion by the teager-kaiser energy operator, JASA 135 (6) (2014) 258–264.
[36] S.A. Khoubrouy, I.M.S. Panahi, J.H.L. Hansen, Howling detection in hearing aids based on generalized teager-kaiser operator, IEEE TASPL 23 (1) (2015) 154–161.
[37] A. Tigrini, A. Mengarelli, S. Cardarelli, S. Fioretti, F. Verdini, Improving EMG signal change point detection for low SNR by using extended teager-kaiser energy operator, IEEE TMRB, 2 (4) (2020) 661–669.
[38] W. Lin, P. Chitrapu, Time-frequency distributions based on teager-kaiser energy function, Conf. IEEE ICASSP, 3 (1996) 1818–1821.
[39] A.O. Boudraa, Relationships between ψ_b-energy operator and some time-frequency representations, IEEE SPL., 17 (6) (2010) 527–530.
[40] A. Bouchikhi, A.O. Boudraa, J.C.C.T. Chonavel, Analysis of multicomponent LFM signals by a combined teager-huang-hough transform, IEEE TAES, 50 (2) (2014) 1222–1233.
[41] R.A. Thuraisingham, Estimation of teager energy using the hilbert huang transform, IET SP, 9 (1) (2015) 82–87.
[42] A.O. Boudraa, E.H.S. Diop, Image contrast enhancement based on 2d teager-kaiser operator, Conf. IEEE ICIP, (2008) 3180–3183.
[43] A.O. Boudraa, E.H.S. Diop, A. Bouchikhi, Teager-kaiser energy bilevel thresholding, Conf. IEEE ISCCSP, (2008) 1086–1090.
[44] J.C. Cexus, A.O. Boudraa, A. Baussard, F.H. Ardeyeh, E.H.S. Diop, 2d cross-ψ_b-energy operator for images analysis, Conf. IEEE ISCCSP, (2010) 1–5.
[45] Y. Attaf, A. Adnane, M. Lahdir, A.O. Boudraa, M. Laghrouche, Z. Ameur, An AM-FM based image segmentation: detection of clouds in MSG images of algeria, Int. Rev. Comput. Soft. 10 (7) (2015) 789–797.
[46] A.O. Boudraa, F. Salzenstein, Teager-kaiser energy methods for signal and image analysis: A review, Digital Sig. Proc., 78 (2018) 338–375.
[47] A.C. Bovik, P. Maragos, Conditions for positivity of an energy operator, IEEE TSP, 42 (1994) 469–471.

[48] K.G. Larkin, On the positivity of an energy operator, Occasional Texts in the Pursuit of Clarity and Simplicity in Research. Series 1 2 (2015) 1–5.
[49] P.K. Banerjee, N.B. Chakrabarti, Noise sensitivity of teager-kaiser energy operators and their ratios, Proc. ICACCI, (2015) 2265–2271.
[50] F. Salzenstein, A.O. Boudraa, J.C. Cexus, Generalized higher-order nonlinear energy operators, JOSA A 24 (2007) 3717–3727.
[51] J.-C. Cexus, A.O. Boudraa, Nonstationary signals analysis by teager-huang transform (THT), Proc. EUSIPCO (2006) 1–5.
[52] E.H.S. Diop, A.O. Boudraa, F. Salzenstein, Higher order teager-kaiser operators for image analysis: Part i. a monocomponent image demodulation, Proc. ICASSP, (2009) 1041–1044.
[53] A.O. Boudraa, J.C. Cexus, H. Zaidi, Functional segmentation of dynamic nuclear images by cross-ψ_b-energy operator, Computer Methods and Programs in Biomedicine, 84 (2006) 146–152.
[54] A.O. Boudraa, J.C. Cexus, M. Groussat, P. Brunagel, An energy-based similarity measure for time series, EURASIP J. Adv. Sig. Proc. 8(2008). Article ID 135892.
[55] J.P. Montillet, On a novel approach to decompose finite energy functions by energy operators and its application to the general wave equation, Int. Math. Forum, 5 (48) (2010) 2387–2400.
[56] B. Santhanam, On a matrix framework for the teager-kaiser energy operator, Proc. IEEE DSP/SPE, (2013) 69–73.
[57] A.O. Boudraa, Y. Préaux, J.C. Cexus, et I. Fujino, Mesure de similarité de signaux par opérateur d'énergie croisée, Proc. GRETSI (2017) 1–4.
[58] A. Javaheri, M.B. Shamsollahi, On higher order positive differential energy operator, ArXiv:1701.03834v.
[59] E. Chassande-Mottin, P. Flandrin, On the time-frequency detection of chirps, ACHA, 6 (2) (1999) 252–281.
[60] A. Savitzky, M.J.E. Golay, Smoothing and dierentiation of data by simplied least squares procedures, Anal. Chem., 36 (8) (1964) 1627–1639.
[61] A.O. Boudraa, Instantaneous frequency estimation of FM signals by cross-ψ_b energy operator, Electron. Lett., 47 (10) (2011) 623–624.